AKADÉMIAI KIADÓ

A new protocol for radio frequency heating of low-moisture, viscous sauces and its temperature uniformity optimisation

H.J. Shi[1], X.B. Li[2*] and Z.M. Yan[3]

[1] College of Fujian Chuanzheng Communications, Fuzhou, Fujian, 350007, China

[2] College of Mechanical and Electrical Engineering, Fujian Agriculture and Forestry University, Fuzhou, 350002, China

[3] College of Food Science and Technology, Fujian Agriculture and Forestry University, Fuzhou, 350002, China

ORIGINAL RESEARCH PAPER

Check for updates

ABSTRACT

Radio frequency (RF) heating of agri-food, especially low moisture viscous sauces (LMVS), have obvious advantages. However, uneven heating is one main problem of RF heating technology that has to be solved. Due to the unclear heating mechanism and the difficulty to measure the three-dimensional temperature distribution in the heated object, computer-aided analysis method was adopted. Based on the RF heating numerical calculation model after experimental verification and the characteristics of polyetherimide (PEI) assisted RF heating of peanut butter (PB), this study proposed an improved method for an existing protocol. Meanwhile, parameters of the new protocol were optimised by the Multi-objective Global Optimisation (MGO) of its surrogate model. Results demonstrated that the best size of PEI block in the new protocol was $\Phi100 \times 9.5$ mm and the positional height was 12 mm. When the pasteurisation temperature Tp was set to 70 °C and the control temperature Tc was set to 75 °C, the temperature uniformity evaluation indices, Over-shoot Temperature Control Index (OTCI) and Targeted Penetration Depth (TPD), were 0.920% and 3.975 mm, respectively. Compared with 4.845% and 4.940 mm before improvement, the new protocol achieved significant optimisation and improved the temperature uniformity effectively. This also proved the feasibility of MGO method of surrogate model in relevant studies.

---

* Corresponding author. Tel.: +86 17720798726. E-mail: cau2002@163.com

AKJournals

1. INTRODUCTION

RF refers to the high-frequency (3 kHz ~ 300 MHz) alternating current electromagnetic waves. Due to the fast heating, high penetration depth, selective heating and strongly controllable processing, RF technology is widely applied in agricultural products' insecticidal and food sterilisation. In recent years, food sterilisation based on RF heating became one of the international research hotspots, and it involves fluid food (Geveke et al., 2007), powder products (Ballom et al., 2021), solid food (Cui et al., 2021), etc., especially Low Moisture Viscous Sauces (LMVS). *Salmonella* strains in low-moisture foods can survive for a very long time, their number decreases only by 1 Log after 248 ~ 1,351 d under normal temperature (Podolak et al., 2010). *Salmonella* infection events involve many types of food (Scott et al., 2009) traditionally heat conduction sterilised, which has the disadvantages of low thermal conductivity, long processing time, poor quality, and high energy consumption. Non-thermal sterilisation techniques, such as chemical and radiation sterilisation, might have chemical and radiation residues threatening human health. Ultra-high Static Pressure requires a relatively high water activity and claims a high cost (Goodridge et al., 2006). Infrared and UV sterilisation techniques have small processing area, and they are inapplicable to batch business operations. Verma et al. (2021) confirmed that RF process could be effectively used for pasteurising and drying of basil leaves, and had no significant effect on the quality parameters (colour, total volatiles, total phenolics, and antioxidant activity) of the dried basil leaves.

However, RF heating technology still has the problem of uneven heating, which is caused by the electromagnetic field, the sample, and their interactive factors. The consequences of uneven heating are introduced as follows: On one hand, the heating temperature might be too low as the fear of overheating, leading to quality degradation, might result in inadequate sterilisation intensity. On the other hand, overheating to meet sterilisation requirements damages appearance and quality of the processed object. Previous methods to solve uneven heating of RF include: 1) RF combined with hot air treatment, such as for rice bran (Liao et al., 2020) and white bread (Liu et al., 2011). However, RF heating technique under the assistance of hot air and hot water is not applicable to LMVS with high thermal resistance and increases energy consumption. 2) RF intermittent incentive method (Wang et al., 2013) supposed that temperature was in normal distribution, which had some limitations. 3) Agri-food substitutions (Wang et al., 2014) such as 1% CMC solution and polyurethane foam, though these substitutions are different from physical samples especially in term of response characteristics to the electromagnetic field. 4) Computer simulation. Zhang et al. (2019) showed that computer simulation with geometry obtained by 3D scanning could accurately reproduce the experimental results for the hot/cold spot locations and temperature values. It has obvious advantages in the study of RF heating uniformity due to its improved prediction accuracy.

Due to texture features of the solid-glue-liquid mixture system, RF heating uniformity of LMVS is mainly determined by energy transformation capacity and energy distribution situation of different components in the sample, especially when the thermal resistance and flow

resistance of these components are relatively high. As a result, it is necessary to control heating from energy distribution in the RF field in order to increase temperature uniformity. Jiao et al. (2015) and Shi et al. (2016) used polyetherimide (PEI) as a medium to increase heating uniformity of peanut butter (PB), which is a high-protein and high-lipid LMVS and is consumed widely. Usually, PB is prepacked and ready to eat, which is vulnerable to *Salmonella* infection. Therefore, it is of practical importance to study the temperature uniformity of RF sterilisation of PB. Jiao et al. (2015) studied RF heating uniformity after putting PEI blocks with different diameters (2, 4, 6, 8, and 10 cm) on the upper and lower surfaces of PB, and found that the best uniformity was achieved when PEI diameter was 8 cm. The maximum temperature difference in the whole sample was 9 °C, while the PB temperature difference without PEI was 17 °C. This proved that PEI could increase temperature of cold point in the RF heating process effectively. Shi et al. (2016) proposed the Top and Inner First (TIF) heating pattern and comprehensive evaluation index of temperature uniformity. The TIF heating mode and high heating rate were achieved by keeping samples close to the top electrode and putting PEI block at the bottom of the samples. During RF heating of $\Phi100 \times 50$ mm cylinder PB, the temperature uniformity comprehensive evaluation indices Over-shoot Temperature Control Index (OTCI) and Targeted Penetration Depth (TPD) were 4.845% and 4.940 mm with the distance between electrodes, sample height, and PEI block size below the samples of 84 mm, H = 25.5 mm, and $\Phi80 \times 12.7$ mm, respectively. The target temperature was 70 °C, and the upper limit of temperature control was 75 °C.

PEI influenced energy distribution in the RF heating of PB, but the further studies on the mechanism and control effect need to be carried out. Jiao et al. (2015) and Shi et al. (2016, 2021) had made some progress in related studies, but there may still be other better protocols and parameter optimisation. Therefore, the following work was carried out in this study:

1. Studying better protocol

According to relevant literature studies, the influencing laws of PEI on RF heating of PB were summed up. Better protocol to improve the mode of heating that is the top surface and internal priority heating mode (TIF mode) was proposed based on the above influencing laws, and named as the improved TIF mode.

2. Parameter optimisation

A multi-objective global intelligent optimisation algorithm based on surrogate models was used to determine the optimal parameters of the new protocol.

2. MATERIALS AND METHODS

2.1. Materials

Extensively consumed high-protein and high-lipid PB was chosen to study RF heating uniformity. RF sterilisation has potential application prospects for PB, which is a type of LMVS. In addition, PB is a pre-packaged ready-to-eat food with high nutritional value, good taste, wide consumption range, and a wide range of exposure to bacterial infection events. Therefore, the use of RF sterilisation is of practical significance.

2.2. Methodology

2.2.1. Finite element analysis of RF heating and its experimental verification. The energy in the RF field is distributed in the sample in the form of heat, which corresponds to the temperature distribution of the sample. Currently, researches on RF heating uniformity lack measuring means of real-time and accurate 3D temperatures. Major measuring techniques include thermocouple thermometer, single-point temperature measurement by an optical temperature sensor, and infrared thermal imaging surface temperature measurement. The method of setting up multiple measurement points in the sample suffers from incomplete measurements, difficulty in locating the measurement points, and changes in the dielectric environment of the sample due to the multi-point layout. In hierarchical surface temperature measurement, the real temperature distribution on the separation surface is damaged since the media separation changes the dielectric environment of samples on the hierarchical surfaces and material adhesion occurs during delamination. Hence, it is necessary to study energy distribution or temperature distribution in the RF heating field through numerical analysis. In this study, RF heating process is simulated by the COMSOL software. The computer for model running was configured with i7-2600 CPU, 3.4 GHz Quad-Core Processor, 16 GB memory, and 64-bit Windows 7 operation system. The experimental verification used a free oscillating RF system of 27.12 MHz, 6 kW power, and the temperature was measured by an optical temperature online monitoring instrument. A real-time measurement of temperature-time variation curve at the geometric centre of samples was performed. Temperature distribution on the sample surface after RF heating was collected by an infrared thermal imager. More details can be found in the literature by Jiao et al. (2015) and Shi et al. (2016).

2.2.2. Temperature uniformity evaluation method. There are various evaluation indices for temperature uniformity at present. In the beginning, Neophytou and Metaxas (1998) proposed a normal power density formula and Wang et al. (2005) proposed HUI index. In recent years, most evaluation indices are based on the root-mean-square principle, such as PUI (Tiwari et al., 2011), UI (Alfaifi et al., 2014), and TUI (Jiao et al., 2015). These indices have the following problems: They only considered the deviations between temperatures at all points and the average temperature, which led to calculation of the temperatures between the target temperature and upper limit of temperature control, affecting the accuracy of the calculation results, as they should not be included. Moreover, none of these indices contains distribution information of low-temperature points (lower than the target temperature points). In view of the above two questions, Shi et al. (2016) proposed a comprehensive evaluation index of temperature uniformity, which consisted of two parts: OTCI and TPD.

$$\text{OTCI} = \frac{\int_V [(T - T_c) + |T - T_c|] dV}{2T_p \cdot V} \tag{1}$$

$$\text{TPD} = \max(\text{de}_1, \text{de}_2) \tag{2}$$

The temperature uniformity is better, when numerical values of the two indices are lower. It has some advantages, such as avoiding the pursuit of the same temperature at different sampling points, but requiring all sampling points to be above the target temperature, which is beneficial for engineering applications.

2.2.3. Revised RF heating protocol to improve temperature uniformity. Shi et al. (2021) carried out the analysis on the effect of PEI on energy distribution of RF heating of PB in Fig. 1 and concluded that PEI-assisted RF heating of PB has the following characteristics: (1) Effects of PEI on temperature distribution during RF heating of PB are local. As the size of PEI increases, the region with increasing temperature expands. Given constant thickness of PEI, its radius is expanding gradually and the region with increased temperature expands along the sample radius; otherwise, it expands along the sample thickness. (2) PEI bias (Fig. 1a) and PEI symmetric placing (Fig. 1b) strengthen the RF heating temperature close to PEI. (3) PEI ring setting (Fig. 1c) eliminates or decreases energy accumulation in the region near the circumferential surface of samples effectively.

Figure 2 shows the protocol of TIF heating pattern, which was proposed by Shi et al. (2016). It kept the sample close to the top electrode (Fig. 2a) and put an appropriate size of PEI block at the bottom of sample (Fig. 2b), This protocol has the advantages of fast heating and cold point at external side of sample. In this paper, an improved TIF protocol (Fig. 3) was proposed according to the characteristics of TIF protocol and the influencing effects of PEI on RF heating of PB, trying to solve the problem that there are many low-temperature points in sample periphery regions except the top surface, while maintaining a fast heating rate, so as to improve the temperature uniformity.
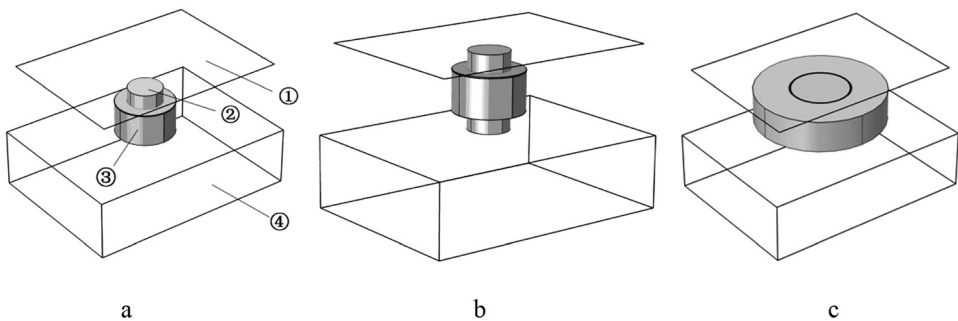

a   b   c

Fig. 1. Three kinds of PEI block positioning to sample (a: on the top surface; b: on the top and bottom surfaces of the sample; c: around the sample). ① Top electrode; ② PEI cylindrical block; ③ Sample: peanut butter; ④ Bottom electrode
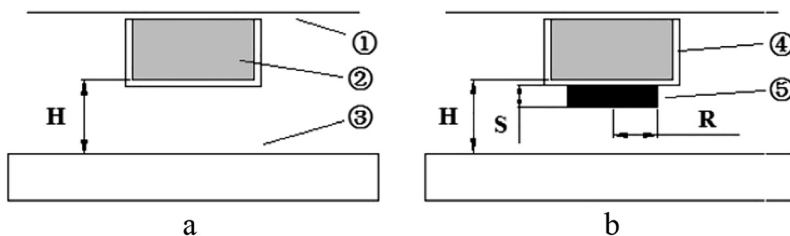

a   b

Fig. 2. Samples were set close to the top electrode of the RF system with an electrode gap of 86 mm (a: without PEI block; b: with PEI block). ① Top electrode ② Peanut butter ③ Bottom electrode ④ Polyethylene container ⑤ Polyetherimide (PEI) block; R: radius of the PEI block; S: thickness of block, H: sample relative height from the bottom electrode
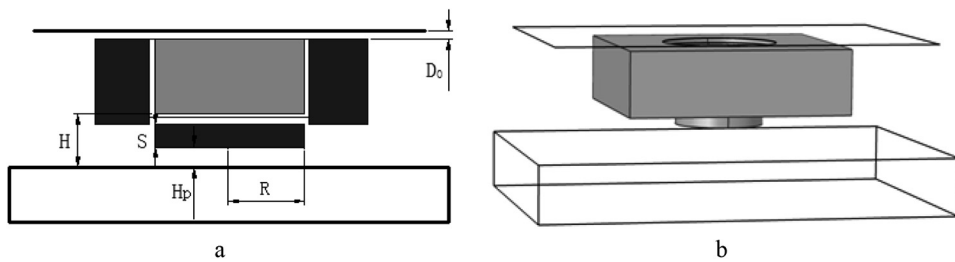
Fig. 3. The improved TIF protocol based on the TIF heating pattern, D_0: distance between the upper surface of the sample and the top electrode; H_P: height of PEI block relative to the bottom electrode. (a: sketch; b: 3D model)

2.2.4. Parameter optimisation based on Multi-objective Global Optimisation (MGO) of surrogate model. Since the RF heating mechanism has not yet been revealed, the mathematical relation between parameters of heating protocol and temperature uniformity is unclear. To study the optimal protocol parameters, surrogate model technology was applied. Meanwhile, the optimisation objectives are the temperature uniformity comprehensive evaluation indices, which include OTCI and TPD, so MGO method was adopted. The surrogate model and MGO were implemented on the ISIGHT software, which is a simulation process automation and multidisciplinary multi-objective optimisation tool. To use this platform, the user needs to do the following: first, create a corresponding workflow; then open the Pointer Optimiser and select the optimisation method, set the variables and their ranges, constraints, and objective functions; and finally, enter the initial points for the optimisation iteration.

3. RESULTS AND DISCUSSION

3.1. Finite element analysis results of improved TIF protocol

To decrease analysis scale, the following parameters were determined preliminarily based on the study of Shi et al. (2016): distance between the electrodes was determined as 86 mm; sample height in relative to the bottom electrode H was 31 mm; the size of peripheral PEI block was $400 \times 246 \times 59$ mm; the radius of the central hole was 52 mm. RF heating continued until the lowest temperature on the top surface of sample reached 70 °C. The parameters to be optimised and analysed were mainly the size of the PEI block below the sample, specifically the radius R, thickness S, and its position height Hp. According to practical situations, the range of these parameters were determined as $40 \leq R \leq 51.5$ mm, $7 \leq S \leq 13$ mm, and $6 \leq Hp \leq 16$ mm. In the actual operation, a space of D_0 should be 5 mm at least. Hence, $S + Hp \leq 26$ mm. To build a surrogate model for RF heating analysis, some testing points were chosen randomly within the range of the above three parameters for optimisation. According to the previous analysis of the numerical model of RF heating by Shi et al. (2016), OTCI and TPD corresponding to each group of test points are listed in Table 1. The pasteurisation temperature Tp was set to 70 °C and the control temperature Tc was set to 75 °C during OTCI calculation.

Table 1. Sampled data for developing surrogate model to study RF temperature uniformity

S (mm)	R (mm)	Hp (mm)	OTCI (%)	TPD (mm)	S (mm)	R (mm)	Hp (mm)	OTCI (%)	TPD (mm)
40	10	10	0.609	6.160	49	10	11	2.293	4.187
40	8	12	0	9.129	49	13	12	2.453	3.748
40	12	12	0.881	7.000	49	10	13	1.713	4.187
40	10	14	1.387	6.08	50	9	8	2.971	4.141
43.5	10.5	11	3.374	4.751	50	12	8	5.376	2.882
45	9	8	2.378	4.865	50	7	11	3.003	4.141
45	12	8	4.503	4.141	50	13	11	5.144	2.577
45	8	10	1.044	5.594	50	8	12	0.102	5.644
45	12	10	3.006	4.455	50	12	12	1.386	4.138
45	10	12	2.106	4.360	50	7	13	3.884	3.971
45	8	14	1.279	4.656	50	13	13	4.678	2.993
45	9	14	2.883	4.672	50	9	14	3.325	3.668
45	12	14	2.928	4.042	50	10	14	1.898	3.893
45	12	14	4.778	3.475	50	12	14	5.460	2.875
47.5	10.5	6	4.055	3.893	51	10	11	2.463	3.893
47.5	8	11	1.296	4.862	51	7	12	0.951	4.656
47.5	10.5	11	3.936	4.075	51	13	12	2.560	3.404
47.5	13	11	5.844	3.078	51	10	13	1.819	4.141
47.5	10.5	16	2.848	3.718	51.5	10.5	11	4.411	3.386

## 3.2. MGO results and verification

The mathematical model of MGO was gained after the above analysis, see Formula 1 for details. Combined with the sample data of the surrogate model in Table 1 and the selected initial point for optimisation being $X_0 = [x_1, x_2, x_3]^T = [45, 11, 13]^T$, the optimal solution after ISIGHT optimisation was $\bar{X} = [50, 9.5, 12]^T$.

Design variables: $\mathbf{X} = \begin{bmatrix} x_1 & x_2 & x_3 \end{bmatrix}^T = \begin{bmatrix} S & R & H_p \end{bmatrix}^T$

$$\left.\begin{aligned} &\min F(\mathbf{X}) = \begin{bmatrix} f_1(\mathbf{X}), f_2(\mathbf{X}) \end{bmatrix}^T = [OTCI, TPD]^T \\ &s.t. \ \ 40 \leq x_1 \leq 51.5 \\ &\qquad 7 \leq x_2 \leq 13 \\ &\qquad 6 \leq x_3 \leq 16 \\ &\qquad 0 \leq f_1(\mathbf{X}) \leq 1.5 \\ &\qquad 0 \leq f_2(\mathbf{X}) \leq 4.5 \\ &\qquad x_1 + x_2 \leq 26 \end{aligned}\right\} \qquad (3)$$

Therefore, finite element analysis and experimental verification were performed by choosing R = 50 mm, S = 9.5 mm, and Hp = 12 mm. Figure 4a shows the temperature distribution of experimental and simulated results on the top surface of PB. Figure 4b shows experimental and simulated time-temperature histories at the centre of the sample. Figure 4c shows the temperature distribution of cross-sectional surface in simulation.
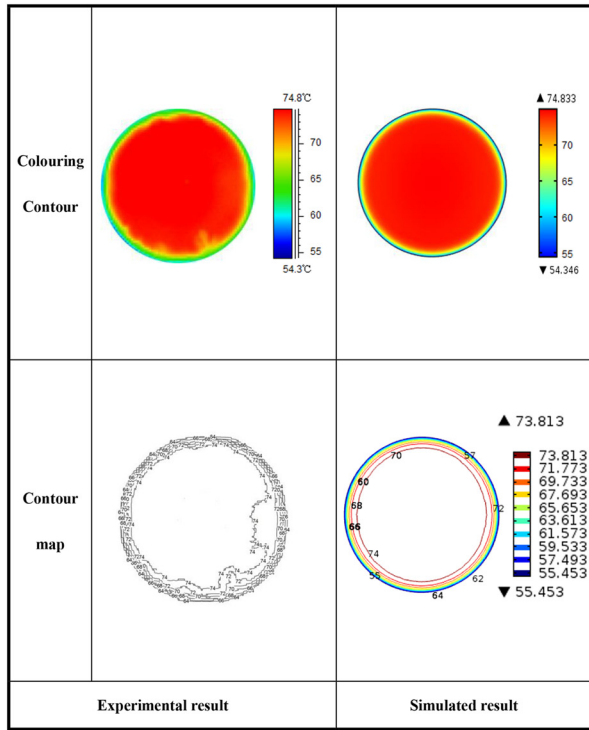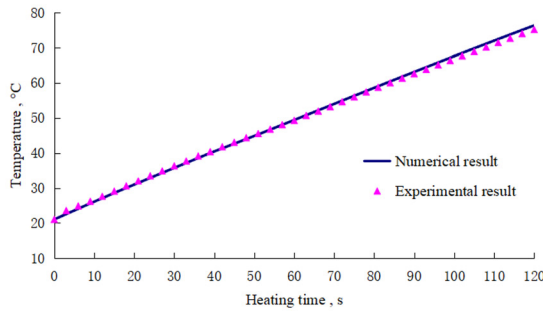
Fig. 4. Simulated and experimental results of the improved TIF protocol based on the parameters of MGO
(a: the temperature distribution and contour on the top surface from simulated model and experiment;
b: heating rate of the physical centre point from simulated model and experiment; c: the temperature
distribution of cross-sectional surface in simulation.)

Based on temperature distribution on top surface and heating rate curve of sample in the central point, the numerical analysis and experimental results agree highly. The abnormal temperature in the experimental results was caused by shaking when samples after RF heating were moved manually from RF cavity to the infrared imager for temperature collection. Looking from the temperature distribution on sample cross section, the whole region showed relatively high temperature uniformity except that the temperature at the edges of the package box was about 20–30 °C lower than the highest temperature. It was calculated that OTCI and TPD were 0.920% and 3.975 mm, respectively. The results were compared with optimisation sample (referring to Table 1). Obviously, $\bar{X} = [50, 9.5, 12]^T$ is the optimal solution. Compared with protocol of Shi et al. (2016), OTCI and TPD were 4.845% and 4.940 mm, respectively, indicating that the optimisation solution increases temperature uniformity greatly.

3.3. Discussion

Numerical analysis and experimental results both reflected that temperature on the sample circumferential side and the bottom surface were relatively lower in the improved TIF protocol, and there was better temperature uniformity on the interior and top surface of the sample compared to the previous scheme (Fig. 2b). Since it usually needs to keep temperature for a period in thermal processing of agri-food, hot water immersion can be adopted to pre-packed PB after RF heating. In this case, temperature on the sample circumferential side and the bottom surface can be raised rapidly to the targeted temperature under the conduction of internal and external temperatures.

In contrast to the study by Jiao et al. (2015), the low temperature point after RF heating is on the top surface and inside the sample, and it is difficult to increase the temperature in this part either by conventional heat transfer methods or other advanced methods. Therefore, this solution has a higher practical value. However, the temperature distribution on the cross section of the sample was not measured in the test, as the fluidity of PB increased after it was heated to more than 70 °C, it was difficult to split the material on the cross section to measure the temperature on the surface. Even if it was split, the measurement result was inaccurate. Therefore, it is necessary to explore an effective measurement method in future test.

4. CONCLUSIONS

From our research results, the following major conclusions could be drawn:

1. PEI assisted RF heating of PB can change temperature distribution in the inner sample, showing some specific influencing treats. It can find the best PEI assisted RF heating protocol *via* simulation.
2. It is feasible to use MGO of surrogate model for parameter optimisation of RF heating protocol. The mechanism of RF heating of agri-foods has not been fully revealed, and in the case that the mathematical relationship between the RF heating parameters and the results has not been established, a surrogate model of the MGO method can be used for relevant studies.
3. As for RF heating of PB contained in a cylindrical box with size of $\Phi 100 \times 50$ mm, the best protocol and parameters obtained in this study are as follows: the distance between electrodes

is 86 mm; the sample is close to the top electrode and PEI blocks are placed around and at the bottom of the sample, with the size of $400 \times 246 \times 59$ and $\Phi 100 \times 9.5$ mm, respectively; position height Hp is 12 mm; the temperature uniformity evaluation indices OTCI and TPD are 0.920% and 3.975 mm, respectively.

ACKNOWLEDGEMENT

REFERENCES

Alfaifi, B., Tang, J., Jiao, Y., Wang, S., Rasco, B., Jiao, S., and Sablani, S. (2014). Radio frequency disinfestation treatments for dried fruit: model development and validation. *Journal of Food Engineering*, 120: 268–276.

Ballom, K., Dhowlaghar, N., Tsai, H.C., Yang, R., and Zhu, M.J. (2021). Radiofrequency pasteurization against *Salmonella* and *Listeria monocytogenes* in cocoa powder. *LWT – Food Science and Technology*, 145(10): 111490.

Cui, B., Fan, R., Ran, C., Yao, Y., and Wang, Y. (2021). Improving radio frequency heating uniformity using a novel rotator for microorganism control and its effect on physiochemical properties of raisins. *Innovative Food Science & Emerging Technologies*, 67(1): 102564.

Geveke, D.J., Brunkhorst, C., and Fan, X. (2007). Radio frequency electric fields processing of orange juice. *Innovative Food Science & Emerging Technologies*, 8(4): 549–554.

Goodridge, L.D., Willford, J., and Kalchayanand, N. (2006). Destruction of *Salmonella* Enteriditis inoculated onto raw almonds by high hydrostatic pressure. *Food Research International*, 39(4): 408–412.

Jiao, Y., Shi, H., Tang, J., Li, F., and Wang, S. (2015). Improvement of radio frequency (RF) heating uniformity on low moisture foods with polyetherimide (PEI) blocks. *Food Research International*, 74(8): 106–114.

Liao, M., Damayanti, W., Xu, Y., Zhao, Y., and Jiao, S. (2020). Hot air-assisted radio frequency heating for stabilization of rice bran: enzyme activity, phenolic content, antioxidant activity and microstructure. *LWT – Food Science and Technology*, 131: 109754.

Liu, Y., Tang, J., Mao, Z., Mah, J.H., Jiao, S., and Wang, S. (2011). Quality and mold control of enriched white bread by combined radio frequency and hot air treatment. *Journal of Food Engineering*, 104(4): 492–498.

Neophytou, R.I. and Metaxas, A.C. (1998). Combined 3D FE and circuit modeling of radio frequency heating systems. *Journal of Microwave Power and Electromagnetic Energy*, 33(4): 243–262.

Podolak, R., Enache, E., Stone, W., Black, D.G., and Elliott, P.H. (2010). Sources and risk factors for contamination, survival, persistence, and heat resistance of *Salmonella* in low-moisture foods. *Journal of Food Protection*, 73(10): 1919–1936.

Scott, V.N., Chen, Y., Freier, T.A., Kuehm, J., Moorman, M., Meyer, J., Morille-Hinds, T., Post, L., Smoot, L., Hood, S., Shebuski, J., and Banks, J. (2009). Control of *Salmonella* in low-moisture foods. I. Minimizing entry of *Salmonella* into a processing facility. *Food Protection Trends*, 29(6): 342–353.

Shi, H., Chen, H., and Yan, Z. (2021). Analysis on the effect of polyetherimide on energy distribution of radio frequency heating of viscous sauce. *International Journal of Food Engineering*, 17(8): 655–664.

Shi, H., Jiao, Y., Tang, J., Zhang, S., and Kuang, P. (2016). Heating uniformity evaluation and improvement of radio frequency treated prepackaged food. *Transactions of the American Society of Agricultural Engineers*, 59(5): 1441–1450.

Tiwari, G., Wang, S., Tang, J., and Birla, S.L. (2011). Analysis of radio frequency (RF) power distribution in dry food materials. *Journal of Food Engineering*, 104(4): 548–556.

Verma, T., Chaves, B.D., Irmak, S., and Subbiah, J. (2021). Pasteurization of dried basil leaves using radio frequency heating: a microbial challenge study and quality analysis. *Food Control*, 124(2): 107932.

Wang, Y., Li, Z., Gao, M., Tang, J., and Wang, S. (2014). Evaluating radio frequency heating uniformity using polyurethane foams. *Journal of Food Engineering*, 136(9): 28–33.

Wang, S., Tang, J., Johnson, J.A., and Cavalieri, R.P. (2013). Heating uniformity and differential heating of insects in almonds associated with radio frequency energy. *Journal of Stored Products Research*, 55: 15–20.

Wang, S., Yue, J., Tang, J., and Chen, B. (2005). Mathematical modelling of heating uniformity for in-shell walnuts subjected to radio frequency treatments with intermittent stirrings. *Postharvest Biology and Technology*, 35(1): 97–107.

Zhang, S., Ramaswamy, H.S., and Wang, S. (2019). Computer simulation modelling, evaluation and optimisation of radio frequency (RF) heating uniformity for peanut pasteurisation process. *Biosystems Engineering*, 184: 101–110.